



Optimal formation of uniform-phase supported lipid bilayers from phospholipid–monoglyceride bicellar mixtures



Tun Naw Sut^{a,b}, Soohyun Park^a, Bo Kyeong Yoon^b, Joshua A. Jackman^{b,*}, Nam-Joon Cho^{a,*}

^aSchool of Materials Science and Engineering, Nanyang Technological University, 50 Nanyang Avenue, 639798, Singapore

^bSchool of Chemical Engineering, Sungkyunkwan University, Suwon 16419, Republic of Korea

ARTICLE INFO

Article history:

Received 18 March 2020

Received in revised form 7 April 2020

Accepted 26 April 2020

Available online 8 May 2020

Keywords:

Supported lipid bilayer

Molecular self-assembly

Bicelle

Phospholipids

Monocaprin

Quartz crystal microbalance-dissipation

ABSTRACT

Supported lipid bilayers (SLBs) spanning hydrophilic surfaces are industrially attractive biomimetic coatings that mimic critical aspects of lipid membrane interfaces and are increasingly used in applications spanning medicine, biotechnology, and environmental science. The use of adsorbing bicelle lipid nanostructures composed of long- and short-chain phospholipid mixtures is an effective self-assembly driven process for streamlined SLB fabrication. However, existing studies use synthetic short-chain phospholipids as a necessary bicelle component and such materials are not practical for industrial applications. Herein, we investigated optimal conditions to fabricate SLBs from bicelles containing an industrially useful monoglyceride called monocaprin (MC) in place of short-chain phospholipids. The ratio of long-chain phospholipid to MC along with total lipid concentration were systematically tested. Quartz crystal microbalance-dissipation (QCM-D) and time-lapse fluorescence microscopy experiments were performed to characterize bicelle adsorption onto silicon dioxide surfaces, and fluorescence recovery after photobleaching (FRAP) measurements were conducted to evaluate lateral lipid diffusion within the fabricated lipid adlayers. Depending on bicelle parameters, high-quality SLB formation with uniform phase properties was achieved and optimal ranges are described to ensure target performance outcomes without phase separation. Together, our findings demonstrate that MC-containing bicelles are useful tools to form high-quality SLBs suitable for surface coating and biosensing applications.

© 2020 The Korean Society of Industrial and Engineering Chemistry. Published by Elsevier B.V. All rights reserved.

Introduction

As biocompatible coatings on solid surfaces, ultrathin supported lipid bilayers (SLBs) are excellent cell membrane mimics [1–3] that can be incorporated as functional elements into highly sensitive, surface-based measurement devices [4,5]. Aside from fundamental research into membrane biology, SLBs have proven useful for various surface coating and sensing applications across the biomedical [6–9], environmental [10–12], and food [13–15] sectors. SLB fabrication generally involves a bottom-up nano-architectonic strategy whereby higher-order lipid bilayer nanostructures are built from the self-assembly of individual lipid molecules [16–19]. Currently, the most widely used method to fabricate SLBs is the vesicle fusion method in which spherical lipid vesicles adsorb and rupture spontaneously on a target surface to form a two-dimensional SLB [20]. However, the vesicle fusion

method has some limitations related to sample preparation, lipid composition, and material support compatibility, which has led to exploring other streamlined, industrially viable SLB fabrication methods [21].

To this end, the use of bicelles, which are typically regarded as disk-like lipid nanostructures made from a mixture of long- and short-chain phospholipids [22,23], offers excellent promise for SLB fabrication. The classical view is that disk-like bicelles are formed by long-chain phospholipids that self-assemble into a bilayer structure and short-chain phospholipids that form a rim around the bilayer edges. There is also growing attention to the wide range of nanostructure morphologies that bicelles can possess depending on factors such as q-ratio (ratio of long- to short-chain phospholipid concentrations), total lipid concentration, and temperature [24–26]. The primary use of bicelles has been in the structural biology field as membrane protein hosts [27–29], and they were recently used in the interfacial science field as an effective SLB fabrication tool. Zeineldin et al. first demonstrated successful SLB fabrication by depositing bicelles on oxidized silicon substrates [30]. Other research groups have since investigated the mechanism of bicelle-mediated SLB formation [31–34] and the

* Corresponding authors.

E-mail addresses: jjackman@skku.edu (J.A. Jackman), njcho@ntu.edu.sg (N.-J. Cho).

results demonstrate the practical utility of bicelles, sometimes also considered as bicellar mixtures in order to reflect the range of possible morphologies, as an alternative to other conventional SLB fabrication approaches. Systematic investigations have been carried out to determine how the total lipid concentration and q -ratio affect SLB formation, and it was determined that optimal SLB conditions occur with lower total lipid concentrations, under which conditions the membrane-destabilizing effects of short-chain phospholipids are minimized [35]. Furthermore, it has been demonstrated that charged bicelles can adsorb and form SLBs on different oxide substrates [36] and the bicelle-mediated SLB formation process works across low and high ionic strength conditions [37]. It has also been possible to incorporate cholesterol into the bilayer region of bicelles and the cholesterol-containing bicelles could adsorb onto silicon dioxide surfaces [38]. The results showed that cholesterol-enriched SLBs can be formed from bicelles with high cholesterol fractions, which enables the fabrication of more biologically relevant SLBs alongside other emerging techniques such as the solvent-assisted lipid bilayer (SALB) method [21,39]. With this demonstrated promise, it is thus important to further explore how bicelle components can be tailored to broaden SLB application opportunities.

Within this scope, there has been scant attention to certain key design components of bicelles for SLB fabrication, especially the short-chain phospholipid component, which has limited the scope of fabrication possibilities while also leaving open the door to develop more practical bicelle options based on industrially applicable, abundant lipid resources. Indeed, although various long-chain phospholipids [e.g., dimyristoylphosphatidylcholine (DMPC) [31], 1-palmitoyl-2-oleoyl-*sn*-glycero-3-phosphocholine (POPC) [32] and 1,2-dioleoyl-*sn*-glycero-3-phosphocholine (DOPC) [35]] have been used to make bicelles, only two types of short-chain phospholipids have been used: 1,2-dihexanoyl-*sn*-glycero-3-phosphocholine (DHPC₆) [31–34] and 1,2-diheptanoyl-*sn*-glycero-3-phosphocholine (DHPC₇) [30,32], which are generally known as DHPC. Aside from short-chain phospholipids, it is also possible to fabricate bicelles with detergent and detergent-like molecules in some cases although such possibilities require exploration for bicelle-mediated SLB fabrication.

One promising option to replace DHPC is the class of monoglycerides which are relatively short-chain lipids that are esterified adducts of a fatty acid and glycerol molecule. Among different monoglycerides, monocaprin (MC) is already widely used in nanostructured assemblies for biotechnology applications such as hydrogels, lipid nanocapsules, and emulsions [40–44]. MC is the medium-chain monoglyceride derivative of the 10-carbon long, saturated fatty acid known as capric acid and is reported to possess potent antibacterial [43,45,46] and antiviral activities [47–49]. Therefore, employing biologically active MC as a molecular component in bicelles could open the door to numerous medical and biotechnology applications while also enabling SLB fabrication from industrially useful lipid combinations.

Herein, our study objective was to fabricate MC-containing bicelles and to identify optimal processing conditions to enable successful SLB fabrication. We prepared bicellar mixtures of DOPC and MC (q -ratios: 0.05, 0.25, 2.5) by using the freeze–thaw–vortex method [35]. The real-time adsorption of DOPC/MC bicelles onto silicon dioxide surfaces was monitored by quartz crystal microbalance-dissipation (QCM-D) and time-lapse fluorescence microscopy, along with fluorescence recovery after photobleaching (FRAP) measurements to measure lateral lipid diffusion, as outlined in Fig. 1. We determined that DOPC/MC bicelles could form SLBs on silicon dioxide surfaces and the optimal conditions in terms of reliable production and uniform phase properties occurred with bicelle parameters of $q = 2.5$ with ≥ 0.063 mM DOPC.

Materials and methods

Reagents

Long-chain phospholipids, 1,2-dioleoyl-*sn*-glycero-3-phosphocholine (DOPC) and fluorescently labeled 1,2-dioleoyl-*sn*-glycero-3-phosphoethanolamine-*N*-(lissamine rhodamine B sulfonyl) (ammonium salt) (Rh-PE), were purchased from Avanti Polar Lipids (Alabaster, AL, USA) and supplied as chloroform stock solutions. Monocaprin (MC) was obtained from LGC Standards (Teddington, UK). The buffer solution used for sample preparation and in all experiments consisted of 10 mM Tris and 150 mM NaCl (pH 7.5), and was prepared using Milli-Q-treated water (MilliporeSigma, Burlington, MA, USA).

Bicelle preparation

A dry lipid film was first formed by placing chloroform dispersed DOPC lipids in a glass vial and exposing the sample to a stream of nitrogen gas for solvent evaporation. The resulting thin film was then stored in a vacuum desiccator overnight to fully remove trace chloroform residues. For fluorescence microscopy and FRAP experiments, 0.5 mol% Rh-PE lipids (with respect to DOPC mol%) were incorporated as well. Next, the dry DOPC or DOPC/Rh-PE film was hydrated to a 1 mM long-chain phospholipid concentration in a buffer that contained 20, 4, or 0.4 mM MC, resulting in bicellar mixture suspensions with $q = 0.05$, 0.25, or 2.5, respectively. These suspensions were then processed using five cycles of freeze–thaw–vortexing, as previously described [35]: freeze in liquid nitrogen for 1 min, thaw in a 60 °C water bath for 5 min, and vortex for 30 s. Bicelle stock solutions were stored at 4 °C and diluted accordingly before experiment.

Quartz crystal microbalance-dissipation (QCM-D)

A Q-Sense E4 instrument (Biolin Scientific AB, Stockholm, Sweden) was used to track bicelle adsorption onto silicon dioxide-coated sensor chips in a label-free measurement format. The sensor chips were prepared for the experiments as follows: clean with water and ethanol, dry with nitrogen gas and treat with oxygen plasma for 1 min in a vacuum chamber (PDC-002, Harrick Plasma, Ithaca, NY). All experiments were conducted at 25 °C and all solutions were injected into the measurement chambers by using a peristaltic pump (Reglo Digital MS-4/6, Ismatec, Wertheim, Germany) at a flow rate of 50 μ L/min. The experimental data were recorded at multiple odd overtones by the Q-Soft software program (Biolin Scientific AB), and the reported data are from the 5th overtone. The data were processed with the Q-Tools (Biolin Scientific AB) and OriginPro (OriginLab, Northampton, MA) software programs.

Time-lapse fluorescence microscopy imaging

A Nikon Eclipse Ti-E inverted microscope with a 60 \times oil-immersion objective (NA 1.49) was used to track bicelle adsorption along with SLB formation in applicable cases. For sample illumination, the emitted light from a mercury-fiber illuminator (C-HGFIE Intensilight; Nikon, Tokyo, Japan) was passed through a TRITC filter. The micrograph images were captured using an Andor iXon3 897 EMCCD camera at the rate of 1 frame per 3 s interval. The sample stage was enclosed within a microfluidic chamber (sticky-Slide VI 0.4, ibidi GmbH, Martinsried, Germany), and experimental samples were injected via peristaltic pump (Reglo Digital MS-4/6) into the chamber at a flow rate of 50 μ L/min. The measurements were performed at ambient room temperature (~ 25 °C).

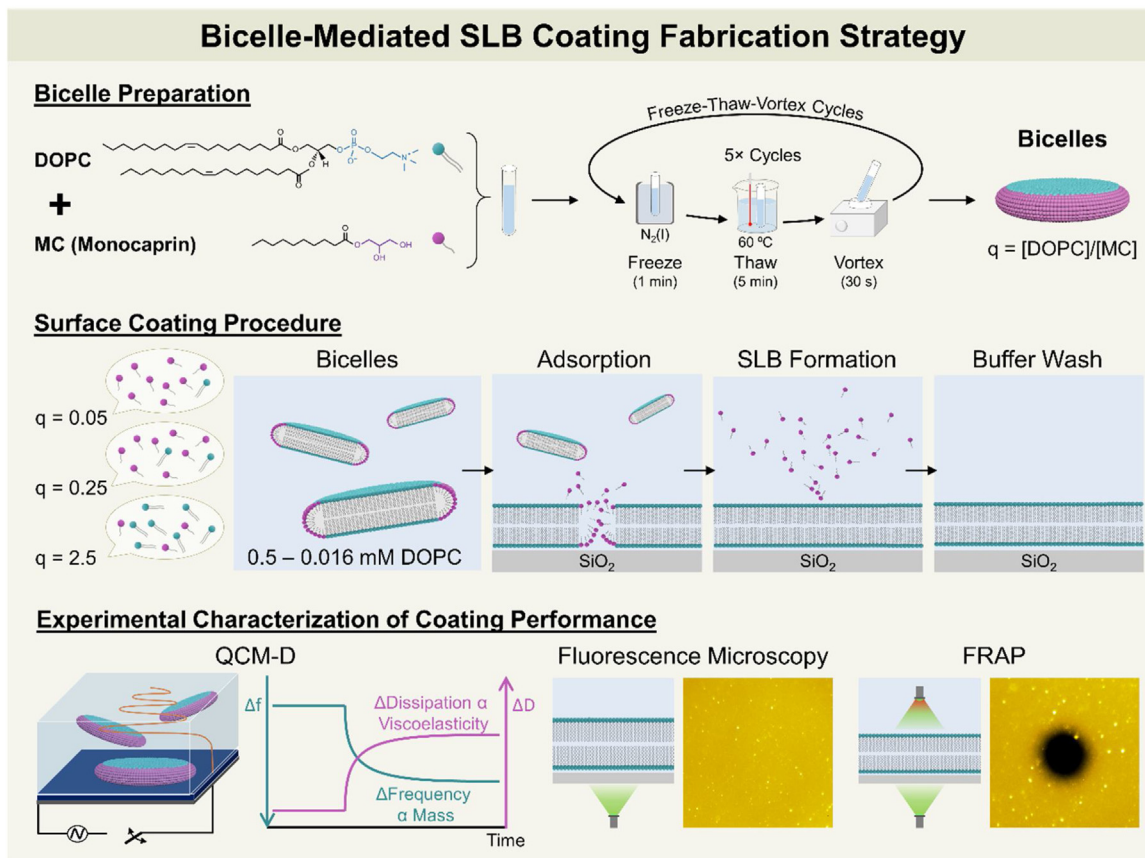


Fig. 1. Optimization of SLB formation using bicellar mixtures of phospholipids and monoglycerides. Bicellar mixtures of DOPC phospholipid and MC monoglyceride were fabricated by hydrating a thin film of dried DOPC lipids in an aqueous buffer containing dispersed MC, followed by five freeze–thaw–vortex cycles. SLB coating performance from fabricated DOPC/MC bicelles was explored systematically as a function of total lipid concentration and q -ratio based on experimental characterization using three surface-sensitive measurement techniques, namely QCM-D, fluorescence microscopy imaging, and FRAP.

Fluorescence recovery after photobleaching (FRAP)

The degree of lateral lipid diffusion within lipid adlayer coatings, resulting from bicelle adsorption processes and buffer washing, was characterized by the FRAP technique. In the experiments, a circular spot of 20 μm diameter was photobleached in the adsorbed lipid layers (irreversible fluorophore quenching within the region) by using a single-mode laser source with 532 nm wavelength and 100 mW power (Coherent Inc., Santa Clara, CA). After photobleaching, time-lapse fluorescence micrographs of that region and the near vicinity were captured every 2 s for a total of 2 min to track fluorescence recovery and the diffusion coefficient of lateral lipid mobility was computed by the Hankel transform method [50].

Results and discussion

Optimization of bicelle parameters for SLB fabrication

We conducted QCM-D experiments to track DOPC/MC bicelle adsorption kinetics onto silicon dioxide surfaces. The QCM-D technique measures the shifts in frequency (Δf) and energy dissipation (ΔD) of silicon dioxide-coated piezoelectric quartz sensors as bicelles adsorb and undergo structural transformations depending on the case. Recorded as a function of time, the Δf and ΔD signals provide information about the real-time changes in mass and viscoelastic properties of the adsorbed layer, respectively [51]. Typically, a decrease in the Δf signal relates to an increase in adsorbed mass, while an increase in the ΔD signal relates to

increasingly viscoelastic properties of the adsorbed film. In the experiments, a baseline signal was first established with buffer solution only before injecting bicelles. Continuous flow-through conditions were maintained during the entire injection period, except to switch between the sample and buffer exchange steps. After bicelle adsorption and/or SLB formation was completed based on the measurement protocol, a buffer wash was performed to remove weakly bound lipid molecules for at least 10 min. The adsorption kinetic profiles as well as the final Δf and ΔD shifts after the washing step were used to determine if SLB formation occurred and thus identify optimal bicelle parameters accordingly. The typical Δf and ΔD values for phospholipid SLBs range around -26 Hz and $<1 \times 10^{-6}$, respectively [51], and were used as general guidelines. It should also be noted that deviations from these values can arise depending on the system specifics such as lipid composition [38] and substrate type [52].

For the QCM-D experiments, the range of total lipid concentrations and q -ratios tested was chosen based on our past work with DOPC/DHPC bicelles [35]. We intended to find the optimal conditions for SLB formation from bicelles with q -ratios of 0.05, 0.25, and 2.5. The results are analyzed below for each q -ratio and presented in Fig. 2. For simplicity, only the DOPC concentration is reported (the corresponding MC concentration can be calculated from the q -ratio).

$q = 0.05$

Bicelle adsorption at all test concentrations resulted in no SLB formation (Fig. 2A,B). The bicelles ruptured after reaching a critical surface coverage at 0.5–0.031 mM DOPC, with final Δf and ΔD

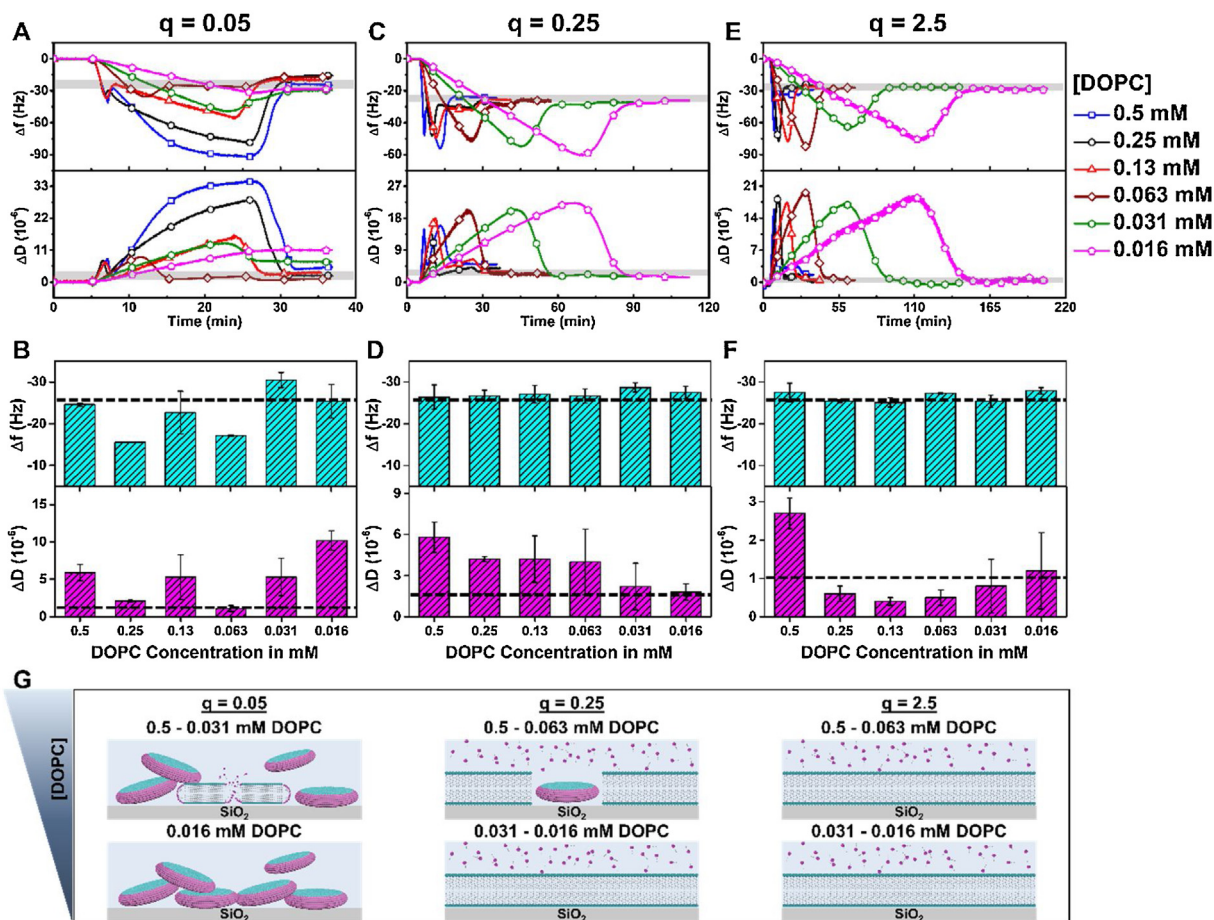


Fig. 2. QCM-D profiling of DOPC/MC bicelle adsorption onto silicon dioxide surfaces as functions of q -ratio and lipid concentration. (A) Frequency and energy dissipation shifts, Δf (top panel) and ΔD (bottom panel), respectively, vs. time, with the grey shaded areas denoting the typical measurement values for a complete SLB, and (B) final Δf (top panel) and ΔD (bottom panel) shifts after buffer wash as a function of lipid concentration, with the dotted lines denoting the mean SLB values, are presented for bicelle adsorption cases at $q = 0.05$. Corresponding data for (C and D) $q = 0.25$ and (E and F) $q = 2.5$ bicelle adsorption cases with equivalent ranges of tested lipid concentrations. (G) Illustrative summary of DOPC/MC bicelle adsorption outcomes at different q -ratios and lipid concentrations.

values around -15 to -30 Hz and 1 to 5×10^{-6} , respectively. In cases of 0.5 – 0.13 mM DOPC, the rupture kinetics indicated detergent-like membrane solubilization effects of MC [53,54], which hindered formation of a high-quality SLB. On the other hand, for the 0.063 – 0.031 mM DOPC cases, MC-induced membrane destabilization effects were not observed. Interestingly, bicelle adsorption at 0.016 mM DOPC was monotonic and reached final Δf and ΔD values around -25.4 ± 4.0 Hz and $10.2 \pm 1.3 \times 10^{-6}$, respectively. While there was evidence of bicelle fusion and rupture, SLB formation did not occur in any of the test conditions. At this q -ratio, the bicelles likely have disk shapes [55] and hence the adsorbed layers probably contain a mixture of intact discoidal bicelles and bilayer patches formed from ruptured bicelles at 0.5 – 0.031 mM DOPC, and only intact discoidal bicelles at 0.016 mM DOPC. Taken together, the results indicate that DOPC/MC bicelles are not suitable for SLB fabrication on silicon dioxide at $q = 0.05$ within all test concentrations.

$q = 0.25$

Bicelle adsorption resulted in SLB formation in some cases at this condition (Fig. 2C,D). In general, the adsorption kinetics showed a two-step mechanism in which the bicelles adsorbed until a critical surface coverage was reached and fusion/rupture occurred [35]. At 0.5 mM DOPC, there was a complex interaction profile associated with bicelle fusion, as indicated by decreasing Δf shifts and increasing ΔD shifts after the rupture process started,

which is suggestive of MC-induced membrane destabilization. Between 0.25 – 0.016 mM DOPC, the membrane-destabilizing effect of MC became weaker with decreasing lipid concentration and bicelle fusion and rupture tended to yield incomplete SLBs. The final Δf shifts ranged around -26 to -29 Hz in all cases, and the corresponding ΔD shifts were around 4 to 6×10^{-6} at 0.5 – 0.063 mM DOPC and around 1 to 3×10^{-6} at 0.031 and 0.016 mM DOPC. Thus, the data support incomplete SLB formation at $q = 0.25$ while the resulting lipid adlayers tended to have more SLB-like properties when formed at lower total lipid concentrations. As at $q = 0.05$, bicelles also likely assemble into a disk shape at $q = 0.25$ [55,56] and therefore, the SLBs likely contain some unruptured bicellar disks at 0.5 – 0.063 mM DOPC, as indicated by high ΔD shifts. Altogether, the results demonstrate that DOPC/MC bicelles at $q = 0.25$ can adsorb and rupture on silicon dioxide surfaces and form incomplete SLBs at lower lipid concentrations.

$q = 2.5$

Bicelle adsorption led to SLB formation via two-step adsorption kinetics for all tested lipid concentrations (Fig. 2E,F). Very mild MC-induced effects were observed between 0.5 – 0.13 mM DOPC and SLB formation proceeded without hindrance from such effects at 0.063 – 0.016 mM DOPC. The final Δf values in all adsorption cases were around -25 to -28 Hz, and ΔD values around $2.7 \pm 0.4 \times 10^{-6}$ at 0.5 mM DOPC and around 0.4 to 1.2×10^{-6} at 0.25 – 0.016 mM DOPC. Interestingly, the best-quality SLBs were formed at 0.13 mM

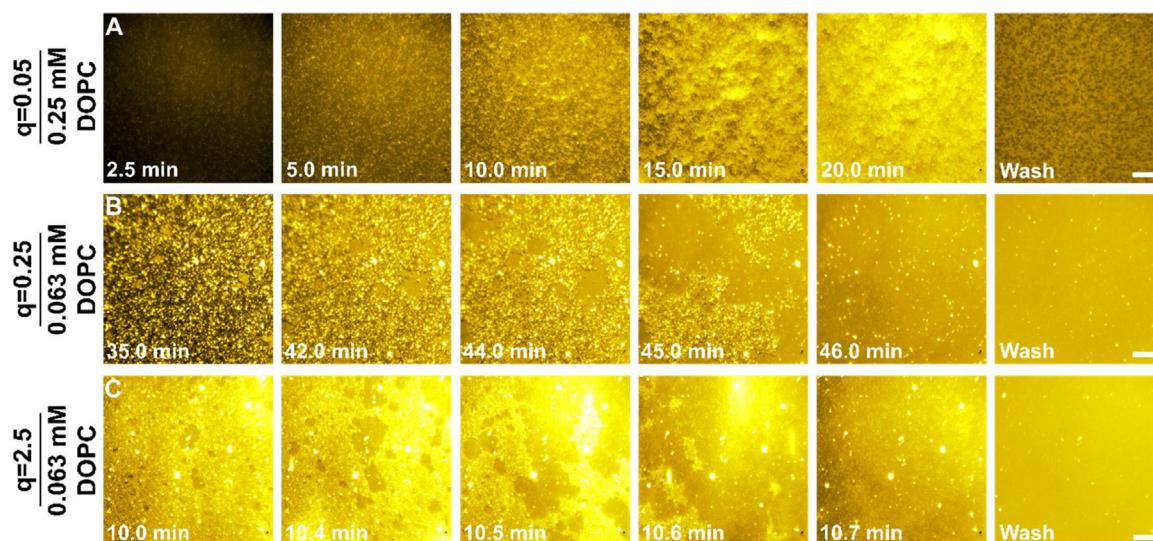


Fig. 3. Real-time fluorescence microscopy observation of DOPC/MC bicelle adsorption and resulting structural transformation processes. Time-lapse fluorescence microscopy images were recorded after adding fluorescently labeled bicelles into the microfluidic chamber. The following bicelle samples were tested: (A) $q = 0.05$ at 0.25 mM DOPC; (B) $q = 0.25$ at 0.063 mM DOPC; and (C) $q = 2.5$ at 0.063 mM DOPC. Scale bars: 20 μm .

DOPC, supporting that there is an optimal lipid concentration that is in an intermediate range. Compared to $q = 0.25$, the formed SLBs had higher quality (since the ΔD shifts are smaller) and the SLB formation appeared to proceed via a more spontaneous rupture process, likely resulting from the adsorption of spherical bicelles that are typical at $q = 2.5$ [57]. Overall, the results show that DOPC/MC bicelles at $q = 2.5$ can form SLBs on silicon dioxide surfaces at all tested lipid concentrations.

To summarize, DOPC/MC bicelles adsorbed and/or ruptured but did not form SLBs at $q = 0.05$ at all test concentrations whereas they formed low-quality SLBs at $q = 0.25$ at low lipid concentrations and high-quality SLBs at $q = 2.5$, especially at intermediate lipid concentrations (Fig. 2G). Altogether, we conclude that the best SLB conditions are at $q = 2.5$ and the concentration range of 0.25–0.063 mM DOPC is optimal as SLBs can be formed with Δf and ΔD values indicative of good coating quality and within an hour at those concentrations.

Since MC is a detergent-like molecule, it is also useful to compare these results with other past attempts to fabricate SLBs using lipid-detergent systems consisting of DOPC lipid and *n*-dodecyl- β -D-maltoside (DDM) detergent [58,59]. From an industrial chemistry perspective, there are some important differences in processing conditions. The DOPC/DDM mixtures likely existed as mixed micelles because they were dispersed in water without any freeze–thaw–vortex processing steps. Additionally, the experimental protocol for SLB fabrication with the DOPC/DDM mixtures involved a series of multiple rinsing steps between adsorption and re-adsorption, whereas our experimental protocol involved only one rinsing step after adsorption. Thus, sample preparation in our case involves additional processing but results in a more streamlined fabrication process overall. Based on our past work with identically processed DOPC/DHPC bicelles [35], the QCM-D data suggest that DOPC/MC mixtures likely have a similar SLB formation mechanism to that system, *i.e.*, bicelles adsorb until a critical surface coverage and fuse/rupture to form an SLB.

Real-time observation of SLB fabrication process

We also performed epifluorescence microscopy experiments to visualize the mechanistic steps involved in bicelle adsorption and SLB formation on a hydrophilic glass surface. We selected particular bicelle parameter cases for each q -ratio in order to

characterize various adsorption scenarios as follows: 0.25 mM DOPC at $q = 0.05$ for adsorption and rupture, and 0.063 mM DOPC at $q = 0.25$ and at $q = 2.5$ for SLB formation. We captured time-lapse micrographs upon injecting fluorescently labeled bicelles into a microfluidic chamber-enclosed glass substrate under continuous flow conditions. The time when the bicelle-containing solution reached the chamber was defined as $t = 0$ min. The results are presented in Fig. 3 and discussed below.

Bicelle adsorbed gradually at $q = 0.05$ at 0.25 mM DOPC, as indicated by an increasing number of bright spots on the surface over time (Fig. 3A). As adsorption continued, the spots started to join together after around 10 min, suggesting bicelle fusion and SLB patch formation. At the same time, bicelles aggregated on the bilayer patches (see the micrograph taken at around 15 min) as more bicelles flowed into the chamber. These aggregates kept forming but disappeared upon buffer washing, leaving a layer of bilayer patches with dark spots. The dark spots appeared to be voids related to MC-induced disruptive effects or possibly fluorophore-poor regions enriched in MC considering that the bulk MC concentration is 20-fold higher than the corresponding bulk DOPC concentration.

Bicelles at $q = 0.25$ and 0.063 mM DOPC adsorbed more slowly and reached the critical surface coverage after around 35 min, followed by rupture with SLB formation occurring within around 11 min thereafter (Fig. 3B). Unlike the aforementioned case, we did not observe MC-induced effects on the SLB in the form of defects in this case, which agrees with the QCM-D measurement data and could be attributed to the lower tested MC concentration at this q -ratio. Nevertheless, a few bright spots remained after buffer washing, indicating the presence of unruptured bicelles in the fabricated SLB.

At $q = 2.5$ and 0.063 mM DOPC, bicelle adsorption was quicker and the critical surface coverage was reached after around 10 min (Fig. 3C). Then, bicelle rupture and bilayer propagation took place quickly, forming an SLB within only 0.7 min. Again, the effects of MC were negligible in this case likely due to the significantly lower MC concentration at this q -ratio, which agrees well with the QCM-D results. After buffer washing, a high-quality SLB was formed as indicated by a uniform fluorescence intensity and only a very small number of bright spots possibly attributed to unruptured bicelles. Together with the QCM-D data, these findings support that DOPC/MC bicelles at $q = 2.5$ enable successful SLB fabrication.

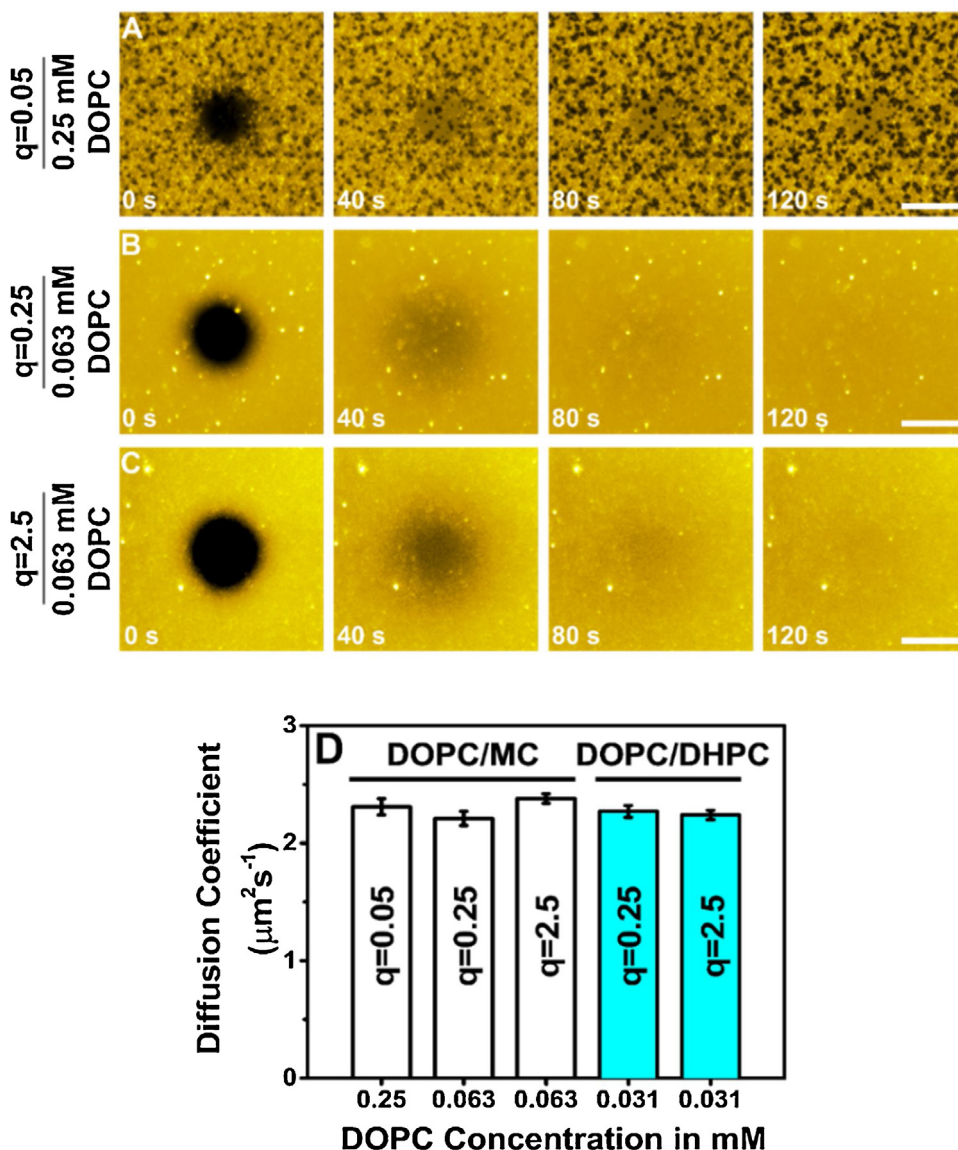


Fig. 4. FRAP results for mobility characterization of lipid adlayers formed at different q-ratios. Upon photobleaching at $t = 0$ s, the fluorescence micrographs were taken while fluorescence recovery occurred within the bleached region, for the next 120 s post-bleaching. The FRAP images are shown for the lipid adlayers formed at the following conditions: (A) $q = 0.05$ at 0.25 mM DOPC; (B) $q = 0.25$ at 0.063 mM DOPC; and (C) $q = 2.5$ at 0.063 mM DOPC. Scale bars: 20 μm . (D) Diffusion coefficients for the lipid adlayers formed from DOPC/MC bicelles or DOPC/DHPC bicelles with the denoted q-ratio and DOPC lipid concentration. The DOPC/DHPC data is from Ref. [35].

Characterization of lateral lipid diffusion within lipid adlayers

FRAP measurements were also performed to determine the lateral diffusion of lipid molecules within adsorbed layers, which is an important property for assessing the biomimetic character of an SLB and related to membrane fluidity. The results are presented in Fig. 4.

The fluorescence intensity within the bleached spot was recovered from adlayers formed using bicelles at $q = 0.05$, demonstrating that lipid molecules within the adlayer are laterally mobile (Fig. 4A). The diffusion coefficient was around $2.31 \pm 0.07 \mu\text{m}^2/\text{s}$, which is similar to the diffusion coefficient of mobile SLBs formed from DOPC/DHPC bicelles [35]. Interestingly, the fluorescence recovery observed in this case suggests that the dark spots are possibly not voids or defects, the presence of which can reduce diffusivity [60,61], but rather comprised of laterally mobile molecules. Moreover, there are two factors which support that MC molecules are present in the fluorophore-poor regions and

indicative of a phase-separated state: (1) MC molecules, being non-ionic surfactants, can intercalate into both leaflets of the lipid bilayer [62]; and (2) the MC molecules are not fluorescently labelled. These two factors also explain the microscopy result where bicelle aggregates on top of bilayer patches (*cf.* Fig. 3A; micrographs at 15 min and 20 min) act as an MC reservoir leading to intercalation of MC molecules into the underlying bilayer and were subsequently removed upon buffer washing. This process left the bilayer with fluorophore-poor, MC-rich phase regions within the SLB that appeared as black spots. Furthermore, the QCM-D result can be explained in the same way; the bicelle aggregates formed on the bilayer (as indicated by the decreasing Δf and increasing ΔD shifts after rupturing in *cf.* Fig. 2A for 0.25 mM DOPC) to allow the MC molecules to intercalate and then desorb after buffer washing, resulting in an SLB with embedded MC molecules for bicelles at $q = 0.05$.

Similar results were obtained for lipid adlayers formed from bicelles at $q = 0.25$ and $q = 2.5$ cases (both at 0.063 mM DOPC); in these

cases, there was nearly complete fluorescence recovery and the diffusion coefficients were $2.21 \pm 0.06 \mu\text{m}^2/\text{s}$ and $2.38 \pm 0.04 \mu\text{m}^2/\text{s}$, respectively, which are within the typical range for SLBs (Fig. 4B,C). The FRAP results also agreed well with past FRAP measurements for SLBs formed from DOPC/DHPC bicelles and plotted for comparison (Fig. 4D). Collectively, the QCM-D, fluorescence microscopy, and FRAP experimental results demonstrate that DOPC/MC bicelles at $q = 2.5$ and with ≥ 0.063 mM DOPC are optimally suitable to form high-quality SLBs on silicon dioxide surfaces.

Conclusion

In this study, we have employed MC as a promising replacement for DHPC to fabricate bicelles and demonstrated the applicability of MC-containing bicelles for streamlined SLB fabrication using industrially practical lipid options. The QCM-D, fluorescence microscopy, and FRAP techniques were utilized to characterize the bicelle adsorption and SLB formation processes. The results showed that DOPC/MC bicelles can form SLBs at $q = 0.25$ and at 2.5 , and optimal formation of uniform-phase SLBs occurred using bicelles at $q = 2.5$ and around $0.25\text{--}0.063$ mM DOPC, where MC-induced destabilization effects were minimal. On the other hand, suboptimal fabrication conditions, depending on bicelle parameters, led to apparently phase-separated SLBs with possible voids triggered by MC-induced membrane disruptive effects or incomplete SLB formation due to the presence of unruptured bicelles still on the surface. Altogether, our findings demonstrate that MC is a useful replacement for DHPC to conduct bicelle-mediated SLB formation and the combination of surface-sensitive measurement techniques used in this work is useful for optimizing the SLB formation process and for conducting quality control assessment of SLB coating properties.

Competing interests

The authors declare that they have no competing interests.

Acknowledgments

This work was supported by the National Research Foundation of Singapore through a Competitive Research Programme grant (NRF-CRP10-2012-07) and a Proof-of-Concept grant (NRF2015NRF-POC0001-19), and by the National Research Foundation of Korea (NRF) grant funded by the Korean government (MSIT) (No. 2020R1C1C1004385).

References

- [1] G.J. Hardy, R. Nayak, S. Zauscher, *Curr. Opin. Colloid Interface Sci.* 18 (2013) 448.
- [2] J.A. Jackman, S.R. Tabaei, Z. Zhao, S. Yorulmaz, N.-J. Cho, *ACS Appl. Mater. Interfaces* 7 (2015) 959.
- [3] H. Su, H.-Y. Liu, A.-M. Pappa, T.C. Hidalgo, P. Cavassin, S. Inal, R.M. Owens, S. Daniel, *ACS Appl. Mater. Interfaces* 11 (2019) 43799.
- [4] J.A. Jackman, A.R. Ferhan, N.-J. Cho, *Bull. Chem. Soc. Jpn.* 92 (2019) 1404.
- [5] J.A. Jackman, N.J. Cho, M. Nishikawa, G. Yoshikawa, T. Mori, L.K. Shrestha, K. Ariga, *Chem. Asian J.* 13 (2018) 3366.
- [6] M.Ö.Ö. Öncel, B. Garipcan, F. İnci, *Biomedical Applications: Liposomes and Supported Lipid Bilayers for Diagnostics, Therapeutics, Imaging, Vaccine Formulation, and Tissue Engineering*, Springer, 2019, pp. 193–212.
- [7] J.F. Verstappen, J. Jin, G. Koçer, M. Haroon, P. Jonkheijm, A.D. Bakker, J. Klein-Nulend, R.T. Jaspers, *J. Biomed. Mater. Res. A* 108 (2020) 923.
- [8] M. Soler, X. Li, A. John-Herpin, J. Schmidt, G. Coukos, H. Altug, *ACS Sens.* 3 (2018) 2286.
- [9] M.A. Elnaggar, D.K. Han, Y.K. Joung, *J. Ind. Eng. Chem.* 80 (2019) 811.
- [10] P. Wagh, I.C. Escobar, *Environ. Progress Sustain. Energy* 38 (2019)e13215.
- [11] Y. Kaufman, A. Berman, V. Freger, *Langmuir* 26 (2010) 7388.
- [12] G.-P. Nikoleli, D. Nikolelis, C.G. Siontorou, S. Karapetis, *Sensors* 18 (2018) 284.
- [13] G.-P. Nikoleli, *Adv. Food Nutr. Res.* 91 (2020) 301.
- [14] J. Gilbert, E.A. Vargas, *J. Toxicol. Toxin Rev.* 22 (2003) 381.
- [15] S. Bratakou, G.P. Nikoleli, C.G. Siontorou, S. Karapetis, D.P. Nikolelis, *N. Tzamtzis, Electroanalysis* 28 (2016) 2171.
- [16] K. Ariga, D.T. Leong, T. Mori, *Adv. Funct. Mater.* 28 (2018)1702905.
- [17] K. Ariga, S. Watanabe, T. Mori, J. Takeya, *NPG Asia Mater.* 10 (2018) 90.
- [18] M. Komiyama, K. Yoshimoto, M. Sisido, K. Ariga, *Bull. Chem. Soc. Jpn.* 90 (2017) 967.
- [19] K. Ariga, T. Mori, J. Li, *Langmuir* 35 (2018) 3585.
- [20] C. Keller, K. Glasmästar, V. Zhdanov, B. Kasemo, *Phys. Rev. Lett.* 84 (2000) 5443.
- [21] J.A. Jackman, N.-J. Cho, *Langmuir* 36 (2020) 1387.
- [22] I. Marcotte, M. Auger, *Concepts Magn. Reson. A* 24 (2005) 17.
- [23] P. Ram, J. Prestegard, *Biochim. Biophys. Acta Biomembr.* 940 (1988) 289.
- [24] L. van Dam, G. Karlsson, K. Edwards, *Biochim. Biophys. Acta Biomembr.* 1664 (2004) 241.
- [25] M.-P. Nieh, V. Raghunathan, C.J. Glinka, T.A. Harroun, G. Pabst, J. Katsaras, *Langmuir* 20 (2004) 7893.
- [26] L. van Dam, G. Karlsson, K. Edwards, *Langmuir* 22 (2006) 3280.
- [27] U.H. Dürr, R. Soong, A. Ramamoorthy, *Progress Nucl. Magn. Reson. Spectrosc.* 69 (2013) 1.
- [28] A.A. De Angelis, S.J. Opella, *Nat. Protoc.* 2 (2007) 2332.
- [29] U.H. Dürr, M. Gildenberg, A. Ramamoorthy, *Chem. Rev.* 112 (2012) 6054.
- [30] R. Zeineldin, J.A. Last, A.L. Slade, L.K. Ista, P. Bisong, M.J. O'Brien, S. Brueck, D.Y. Sasaki, G.P. Lopez, *Langmuir* 22 (2006) 8163.
- [31] S.R. Tabaei, P. Jönsson, M. Brändén, F. Höök, *J. Struct. Biol.* 168 (2009) 200.
- [32] K. Morigaki, S. Kimura, K. Okada, T. Kawasaki, K. Kawasaki, *Langmuir* 28 (2012) 9649.
- [33] Q. Saleem, Z. Zhang, A. Petretic, C.C. Gradinaru, P.M. Macdonald, *Biomacromolecules* 16 (2015) 1032.
- [34] N.L. Yamada, M. Sferrazza, S. Fujinami, *Phys. B Condens. Matter* 551 (2018) 222.
- [35] K. Kolahdouzan, J.A. Jackman, B.K. Yoon, M.C. Kim, M.S. Johal, N.-J. Cho, *Langmuir* 33 (2017) 5052.
- [36] T.N. Sut, J.A. Jackman, N.-J. Cho, *Langmuir* 35 (2019) 8436.
- [37] T.N. Sut, J.A. Jackman, B.K. Yoon, S. Park, K. Kolahdouzan, G.J. Ma, V.P. Zhdanov, N.-J. Cho, *Langmuir* 35 (2019) 10658.
- [38] T.N. Sut, S. Park, Y. Choe, N.-J. Cho, *Langmuir* 35 (2019) 15063.
- [39] S.R. Tabaei, J.-H. Choi, G. Haw Zan, V.P. Zhdanov, N.-J. Cho, *Langmuir* 30 (2014) 10363.
- [40] H. Thormar, G. Bergsson, E. Gunnarsson, G. Georgsson, M. Witvrouw, O. Steingrimsson, E. De Clercq, T. Kristmundsdóttir, *Sex. Transm. Infect.* 75 (1999) 181.
- [41] T. Kristmundsdóttir, S.G. Árnadóttir, G. Bergsson, H. Thormar, *J. Pharm. Sci.* 88 (1999) 1011.
- [42] A. Umerska, V. Cassisa, N. Matougui, M.-L. Joly-Guillou, M. Eveillard, P. Saulnier, *Eur. J. Pharm. Biopharm.* 108 (2016) 100.
- [43] H. Thormar, H. Hilmarsson, G. Bergsson, *Appl. Environ. Microbiol.* 72 (2006) 522.
- [44] J.A. Jackman, B.K. Yoon, D. Li, N.-J. Cho, *Molecules* 21 (2016) 305.
- [45] A.J. Conley, J.J. Kabara, *Antimicrob. Agents Chemother.* 4 (1973) 501.
- [46] B.K. Yoon, J.A. Jackman, E.R. Valle-González, N.-J. Cho, *Int. J. Mol. Sci.* 19 (2018) 1114.
- [47] H. Thormar, C.E. Isaacs, H.R. Brown, M.R. Barshatzky, T. Pessolano, *Antimicrob. Agents Chemother.* 31 (1987) 27.
- [48] H. Thormar, C.E. Isaacs, K.S. Kim, H.R. Brown, *Ann. N. Y. Acad. Sci.* 724 (1994) 465.
- [49] J.A. Jackman, R.D. Boyd, C.C. Elrod, J. Anim. Sci. Biotechnol. 11 (2020) 44.
- [50] P. Jönsson, M.P. Jonsson, J.O. Tegenfeldt, F. Höök, *Biophys. J.* 95 (2008) 5334.
- [51] N.-J. Cho, C.W. Frank, B. Kasemo, F. Höök, *Nat. Protoc.* 5 (2010) 1096.
- [52] S.R. Tabaei, J.A. Jackman, S.-O. Kim, V.P. Zhdanov, N.-J. Cho, *Langmuir* 31 (2015) 3125.
- [53] B.K. Yoon, J.A. Jackman, M.C. Kim, T.N. Sut, N.-J. Cho, *Langmuir* 33 (2017) 2750.
- [54] B.K. Yoon, S. Park, J.A. Jackman, N.-J. Cho, *Appl. Mater. Today* 19 (2020)100598.
- [55] K.J. Glover, J.A. Whiles, G. Wu, N.-J. Yu, R. Deems, J.O. Struppe, R.E. Stark, E.A. Komives, R.R. Vold, *Biophys. J.* 81 (2001) 2163.
- [56] P.A. Luchette, T.N. Vetman, R.S. Prosser, R.E. Hancock, M.-P. Nieh, C.J. Glinka, S. Krueger, J. Katsaras, *Biochim. Biophys. Acta Biomembr.* 1513 (2001) 83.
- [57] M. Shintani, N. Matubayasi, *J. Mol. Liq.* 217 (2016) 62.
- [58] L. Grant, F. Tiberg, *Biophys. J.* 82 (2002) 1373.
- [59] H.P. Vacklin, F. Tiberg, R. Thomas, *Biochim. Biophys. Acta Biomembr.* 1668 (2005) 17.
- [60] P. Nollert, H. Kiefer, F. Jähnig, *Biophys. J.* 69 (1995) 1447.
- [61] N.-J. Cho, L.Y. Hwang, J.J. Solandt, C.W. Frank, *Materials* 6 (2013) 3294.
- [62] H. Heerklott, *Q. Rev. Biophys.* 41 (2008) 205.